ASIAN JOURNAL OF CIVIL ENGINEERING (BHRC) VOL. 17, NO. 4(2016)
PAGES 479-486

ACOUSTIC EMISSION TEST IN VISUALIZING CRACK PROGRESSION FOR CONCRETE BEAMS

J. Ongpeng*
De La Salle University, Manila, Philippines

Received: 20 August 2015; **Accepted:** 28 October 2015

ABSTRACT

In this paper, acoustic emission (AE) test was used to assess concrete beams having a size of 100mm x 100mm x 400mm length with water-cement ratio of 0.50. Two types of beam were considered, plain concrete beams and short steel fiber-reinforced beams. There were three parameters used in acoustic emission test: AE hits, AE location, and AE energy.
The total AE hits were divided into three percentile of AE energy all throughout the test. These are 100th, 25th, and 10th percentile of AE energy. This was done to differentiate significant AE signals with large AE energy from the less significant AE signals with small energy. It was found out that short steel fiber-reinforced concrete beams produced large number of total AE hits compared to ordinary concrete beams. The crack progression was clearly visualized at 10^{th} percentile of AE energy.

Keywords: Non-destructive test; concrete; acoustic emission; fiber-reinforced concrete.

1. INTRODUCTION

Acoustic emission phenomenon is where elastic waves are produced by energy release from a source within a material [1]. A sudden burst of energy in sound waves are generated from developing cracks in a material, and this propagates. These sound waves are received and analyzed using piezoelectric sensor. From previous experiments, crack propagation and micro-cracks with macro deformation of concrete was assessed under uniaxial tension [2]. This test produced good AE signals generated by formation of micro-cracks and dislocation in concrete beams [3].

Damage assessment in masonry structures is very important in monitoring the health of structures. Non-destructive test was carried out in historical masonry building to predict the arrest of crack growth [4]. In order to conduct AE in assessing damage, arrival time and accumulated number of cracks are recorded in the experiment. From oscilloscope, time

*E-mail address of the corresponding author: jason.ongpeng@dlsu.edu.ph (J. Ongpeng)

difference was computed to determine the key parameters in evaluating AE event and location inside a concrete [5,6].

Determination of mode of failure was introduced as damage assessment tool in concrete beams. In an experiment by Ohtsu, crack mouth opening displacement CMOD was related to the damage level according to load and calm ratio [7]. The cracking phenomenon inside the concrete is related to seismic quiescence hypothesis [8]. This hypothesis assumed that main shocks are preceded by seismic quiescence or a stagnant cumulative number of counts before the main shock occur.

In this paper, with the results of AE hits, AE location, and AE energy, a proposed reduction of AE energy according to percentile was used to visualize crack formation inside the damaged concrete when subjected to bending.

2. EXPERIMENTAL PROCEDURE

A total of four beam specimens were casted for ordinary and short steel fiber-reinforced concrete. The size of the specimen is 100mm x 100mm x 400mm. The water-cement ratio used was 0.50. The sand-total aggregate ratio is 45%. Shown in Table 1 is the design mix with 30mm length of steel fiber used.

Table 1: Design mix for the different materials

Item	Max. aggregate size (mm)	W/C (%)	Unit quantity (kg/m^3)				
			Cement	Sand	Gravel	Water- Reducing Agent	Fiber Content
Ordinary concrete	20mm	50	344	761	1038	0.69	0
Fiber-reinforced concrete	20mm	50	344	761	1038	0.69	78.5

After curing all the specimens at 28th day, each specimen was tested using 4-point bending test. The designed loading and unloading path is shown in Fig. 1. The AE test setup is shown in Fig. 2 where six AE sensors were epoxied to the cube at specific points on the surface of the cube. Location of the AE sensors is seen in Table 2. The AE sensors were connected to preamplifier/main amplifier with a factor of 40dB. From the data obtained, viewing of waveforms for six channels was seen in the computer. These data sets were then saved as binary data. Waveform data was processed thru GFORTRAN program to determine the AE hits, AE location, and AE energy.

Table 2: Location of AE sensors

(cm)	x	y	z
ch0	20	7.5	0
ch1	20	2.5	0
ch2	20	10	7.5
ch3	20	10	2.5
ch4	12.75	0	2.5
ch5	27.5	0	7.5

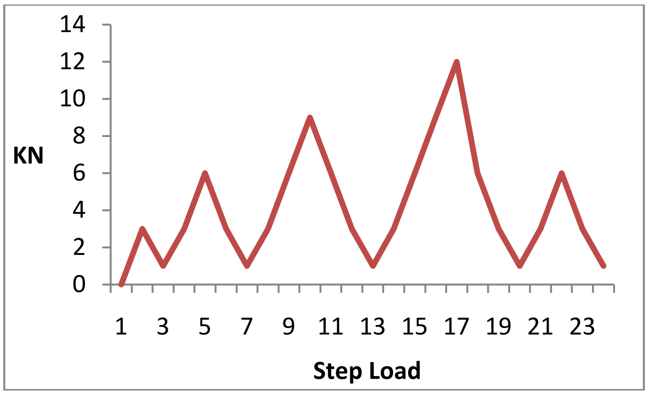

Figure 1. Step load for the beam specimens

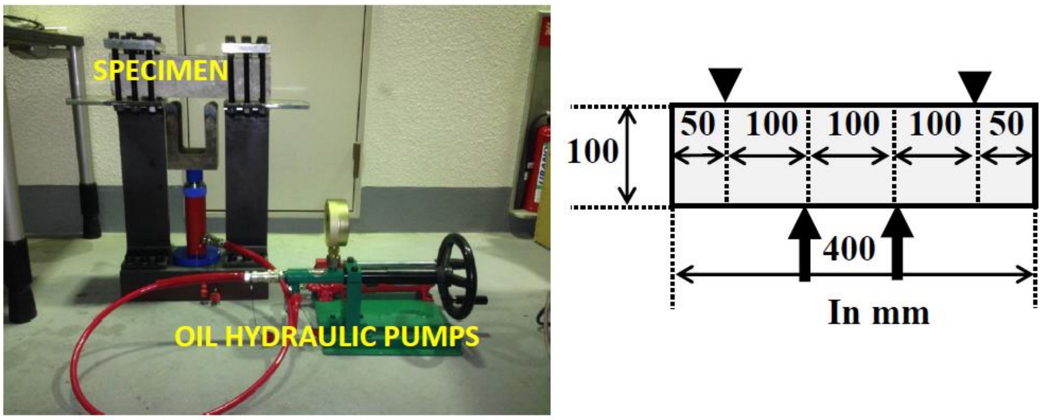

Figure 2. Bending test experimental setup

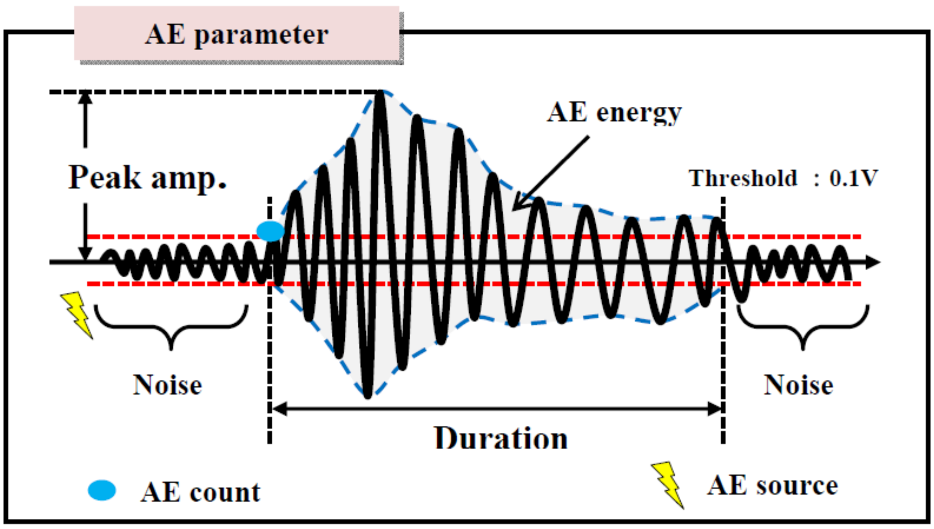

Figure 3. Acoustic emission signal wave parameters

The parameters of AE are shown in Fig. 3 where AE energy was illustrated. Six channels were used in locating the AE source. Eq. 1 represents the distance formula in space of an AE source from AE sensors 1 to 5, while Eq. 2 represents the distance formula in space from AE source to channel 0. The difference of squares for Eq. 1 and Eq. 2 is shown in Eq. 3. Simplifying Eq. 3 will lead to Eq. 4. Repeated calculations were done and convergence to a solution was obtained using least-squares method. The AE energy was computed using Eq. 5.

$$R_i = \sqrt{(x-a_i)^2 + (y-b_i)^2 + (z-c_i)^2} \tag{1}$$
$$R_0 = \sqrt{x^2 + y^2 + z^2} \tag{2}$$
$$R_i - R_0 = v_p t_i \quad (i = 1 \sim 5) \tag{3}$$

where: x, y, z – are the coordinates of the AE source which is unknown
Ri – distance of the AE source to AE sensor channels 1 to 5
Ro – distance of the AE source to AE sensor channel 0
υ_p – Speed of elastic wave in concrete
to – Time from AE source to sensor channel 0
ti – Time difference for all sensor channels (1 to 5) from sensor channel 0

$$\begin{bmatrix} A_{ij} & B_{ij} & C_{ij} \end{bmatrix} \begin{Bmatrix} x \\ y \\ z \end{Bmatrix} = \{ E_{ij} - D_{ij} v_p^2 \} \tag{4}$$

where: $A_{ij} = 2\,(a_i t_j - a_j t_i)$
$B_{ij} = 2\,(b_i t_j - b_j t_i)$
$C_{ij} = 2\,(c_i t_j - c_j t_i)$
$D_{ij} = t_i t_j\,(t_i - t_j)$
$E_{ij} = t_j\,(a_i^2 + b_i^2 + c_i^2) - t_i\,(a_j^2 + b_j^2 + c_j^2)$

$$\text{AE energy} = (R \times \text{Peak amplitude})^2 \times \text{Duration} \tag{5}$$

where: R = distance of AE source location to AE sensors

3. RESULTS AND DISCUSSION

After processing the data using GFORTRAN, the AE results were plotted using MATLAB to show the AE hits, AE location, and AE energy with color map sequence showing the progress of the AE results with respect to load until failure. The total sequence of the color map is the total AE hits experienced when load is increased from 0 to 80%.

In Fig. 4, the 100th percentile or total AE hits were seen. The location of the AE source or micro-cracks was observed. The diameter of the circle in the figure illustrates the AE energy's magnitude. The color of the AE hit represents the sequential progression of AE occurrences. It was found out that ordinary concrete produced less AE hits than fiber-reinforced concrete beam.

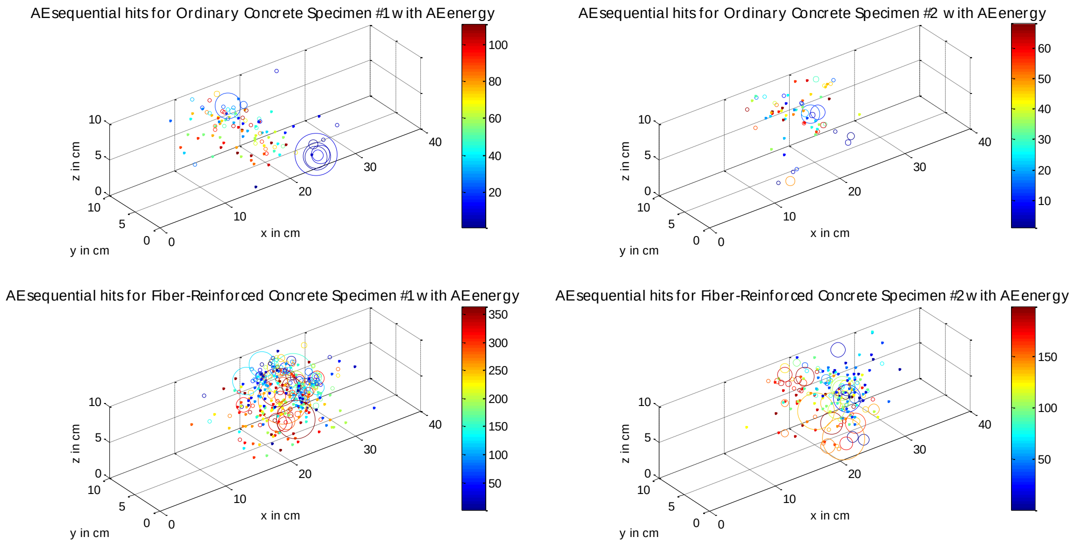

Figure 4. AE energy at 100th percentile

In Fig. 5 and 6, the AE hits were seen for ordinary and fiber-reinforced beam respectively. As seen in the actual picture of the tested specimens, the AE hits visually did not clearly conform to the actual crack formed as shown in the figure. Hence, reduction of AE energy thru 25th percentile and 10th percentile was used to separate significant AE signals with high AE energy.

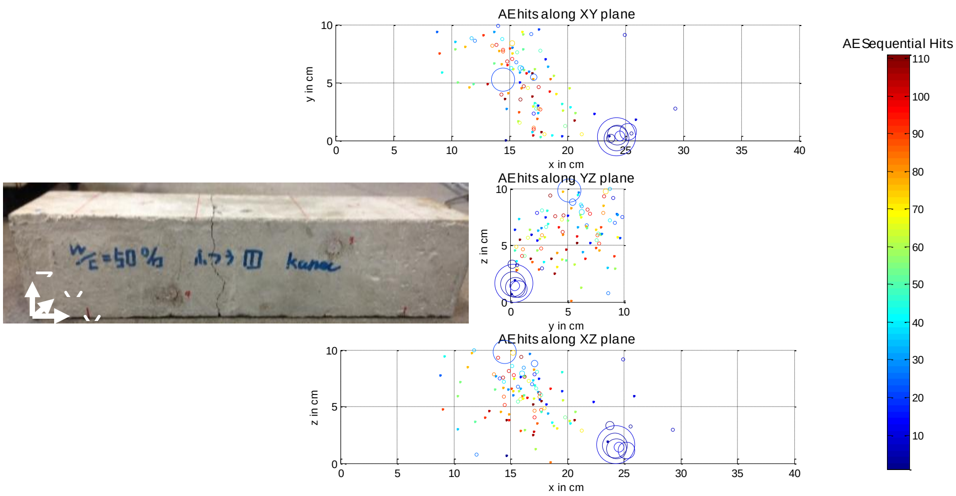

Figure 5. Ordinary concrete beam with 100% AE hits

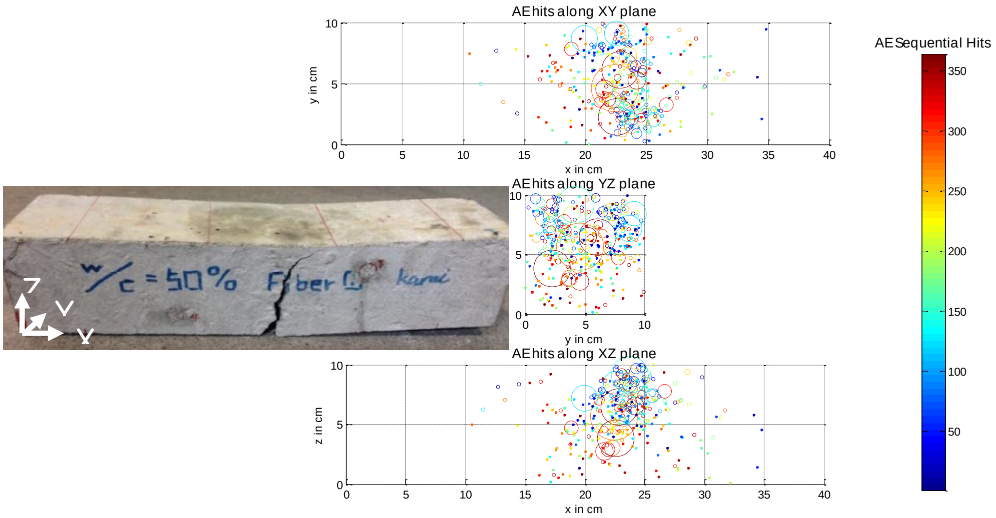

Figure 6. Short steel-fiber concrete beam with 100% AE hits

In Fig. 7, the 25th percentile AE hits were seen. Small AE energy was observed and did not visually match the formed crack after testing. In Fig. 8, the 10th percentile AE hits were seen. This closely conformed to the actual crack formed with significant AE hits and high AE energy.

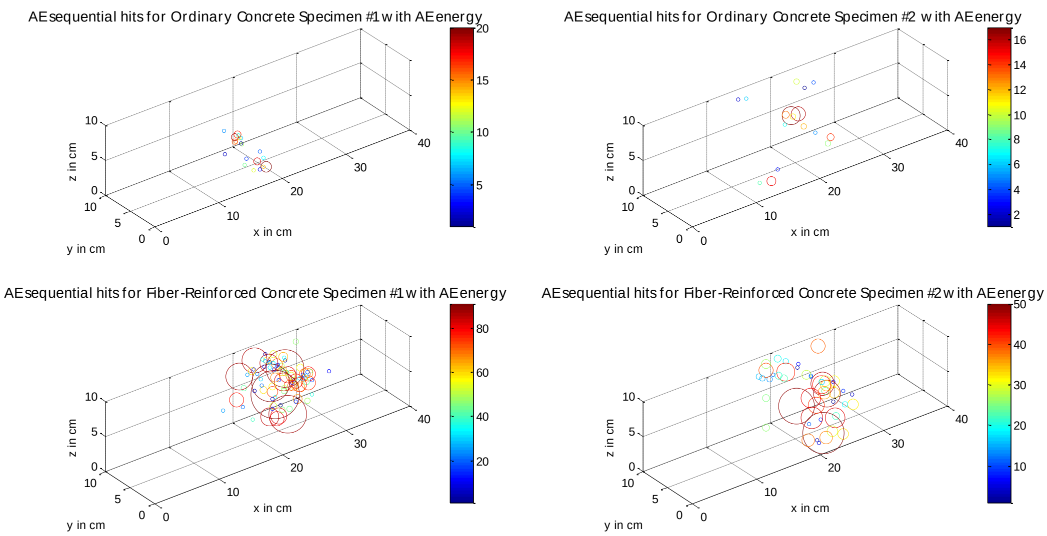

Figure 7. AE energy at 25th percentile

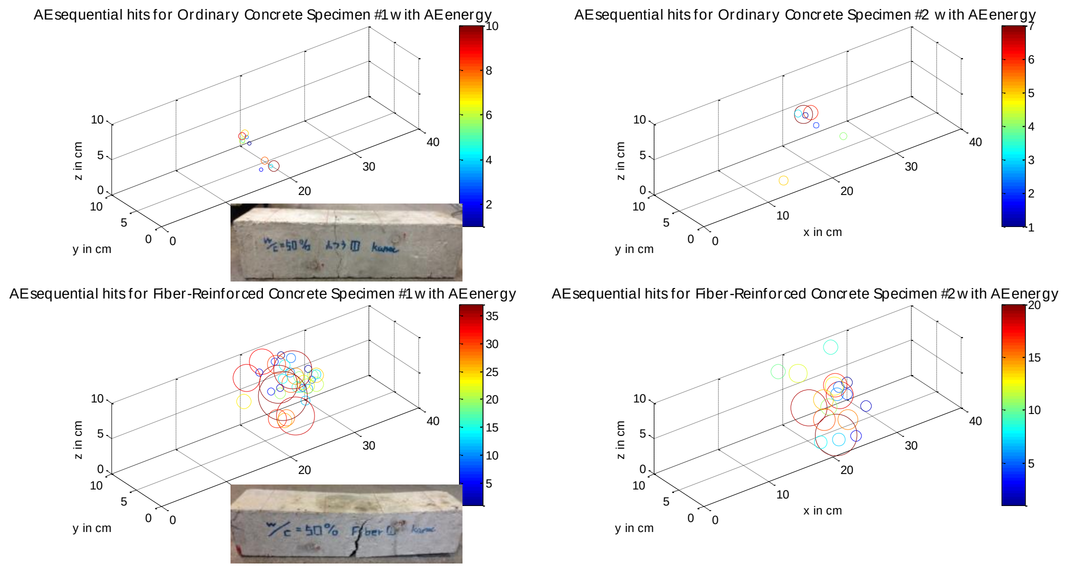

Figure 8. AE energy at 10th Percentile

4. CONCLUSIONS

Acoustic emission (AE) test was used to assess concrete beams crack progression. Three parameters were used in acoustic emission test: AE hits, AE location, and AE energy. The total AE hits were divided into three percentile of AE energy all throughout the test. These are 100th, 25th, and 10th percentile of AE energy.

Reduction of small AE energies to analyze the AE result proved to be efficient in determining the crack formation after testing. This was done to differentiate significant AE signals with large AE energy from the less significant AE signals with small energy.

It was found out that short steel fiber-reinforced concrete beams produced larger number of total AE hits compared to ordinary concrete beams. The crack progression was visualized at 10percentile of AE energy.

Acknowledgments: This work has been supported by Japan Society for Promotion of Science (JSPS) under the Ronpaku Scholarship Program.

REFERENCES

1. ASTM E1316-07b. Standard Terminology for Nondestructive Examinations, ASTM International, West Conshohocken, PA, 2007.
2. Li Z, Shah SP. Localization of microcracking in concrete under uniaxial tension, *ACI Materials Journal*, No. 4, **91**(1994) 372-81.
3. Lu Y, Li Z. Cement-based piezoelectric sensor for acoustic emission detection in concrete structures, *ASCE Earth and Space*, (2008) 1-11.

4. Carpenteri A, Lacidogna G. Damage monitoring of an historical masonry building by the acoustic emission technique, *Materials and Structures*, No. 2, **39**(2006) 161-7.
5. Li Z, Li F, Li X. P-wave arrival determination and AE characterization of concrete, *Journal of Engineering Mechanics*, No. 2, **126**(2000) 194-200.
6. Li Z, Li F, Shah SP. Application of acoustic emission technique to detection of reinforcing steel corrosion in concrete, *ACI Materials Journal*, No. 1, **95**(1998) 68-76.
7. Ohtsu M. The history and development of acoustic emission in concrete engineering, *Concrete Library of JSCE*, **25 (2000)**121-34.
8. Wyss M, Habermann RE. *Precusory Seismic Quiescence*, Springer, **126**(1998) 319-32.